DISSIPATION-INDUCED INSTABILITIES IN MAGNETIZED FLOWS

Oleg N. Kirillov UDC 531.3, 532.5, 537.6

Abstract. We study local instabilities of a differentially rotating viscous flow of electrically conducting incompressible fluid subject to an external azimuthal magnetic field. The hydrodynamically stable flow can be destabilized by the magnetic field both in the ideal and in the viscous and resistive system giving rise to the azimuthal magnetorotational instability. A special solution to the equations of the ideal magnetohydrodynamics characterized by the constant total pressure, the fluid velocity parallel to the direction of the magnetic field, and by the magnetic and kinetic energies that are finite and equal—the Chandrasekhar equipartition solution—is marginally stable in the absence of viscosity and resistivity. Performing a local stability analysis we find the conditions when the azimuthal magnetorotational instability can be interpreted as a dissipation-induced instability of the Chandrasekhar equipartition solution.

CONTENTS

1. Introduction

Dynamics of a flow of a viscous and electrically conducting incompressible fluid that interacts with the magnetic field is described by the Navier-Stokes equation for the fluid velocity $\boldsymbol{u}$ which is coupled with the induction equation for the magnetic field $\boldsymbol{B}$ [14]

$$\begin{aligned} \frac{\partial \boldsymbol{u}}{\partial t}+\boldsymbol{u}\cdot\boldsymbol{\nabla}\boldsymbol{u}-\frac{1}{\mu_0\rho}\boldsymbol{B}\cdot\boldsymbol{\nabla}\boldsymbol{B}+\frac{1}{\rho}\boldsymbol{\nabla}P-\nu\boldsymbol{\nabla}^2\boldsymbol{u} &= 0,\\ \frac{\partial \boldsymbol{B}}{\partial t}+\boldsymbol{u}\cdot\boldsymbol{\nabla}\boldsymbol{B}-\boldsymbol{B}\cdot\boldsymbol{\nabla}\boldsymbol{u}-\eta\boldsymbol{\nabla}^2\boldsymbol{B} &= 0. \end{aligned} \tag{1.1}$$

In the equations (1.1) the total pressure is denoted by $P = p + \frac{\boldsymbol{B}^2}{2\mu_0}$, p is the hydrodynamic pressure, $\rho = const$ is the density, $\nu = const$ is the kinematic viscosity, $\eta = (\mu_0\sigma)^{-1}$ the magnetic diffusivity, σ the conductivity of the fluid, and μ_0 the magnetic permeability of free space. In addition, the incompressible flow and the solenoidal magnetic field fulfil the constraints:

$$\boldsymbol{\nabla}\cdot\boldsymbol{u}=0, \quad \boldsymbol{\nabla}\cdot\boldsymbol{B}=0. \tag{1.2}$$

Let in the steady-state the background flow be differentially rotating in a gap between the radii R_1 and $R_2 > R_1$ with the angular velocity profile $\Omega(R)$ that depends only on the radial coordinate R in the cylindrical coordinate system (R, ϕ, z). Let the background magnetic field have only an azimuthal component with the radial profile $B_\phi^0(R)$, and let the hydrodynamic pressure depend only on R:

$$\boldsymbol{u}_0(R) = R\,\Omega(R)\,\boldsymbol{e}_\phi, \quad p = p_0(R), \quad \boldsymbol{B}_0(R) = B_\phi^0(R)\boldsymbol{e}_\phi. \tag{1.3}$$

,.

In 1956 Chandrasekhar [12] observed that, particularly, $\Omega = \frac{B_\phi^0}{R\sqrt{\rho\mu_0}}$ and $P = constant$ represent an exact stationary solution of the equations (1.1) and (1.2) in the ideal case, i.e. when $\nu = 0$ and $\eta = 0$. On this solution the fluid velocity at every point is parallel to the direction of the magnetic field at that point [14]. Besides, their relative magnitudes are such that the kinetic and magnetic energies are equal: $\frac{\rho(\Omega R)^2}{2} = \frac{(B_\phi^0)^2}{2\mu_0}$. This *equipartition solution* of ideal magnetohydrodynamics was proven by Chandrasekhar to be marginally stable [12, 14]—a bit surprisingly, as he admitted in his memoirs [15]: "One nice result which nevertheless came out at this time was the proof of the stability of the equipartition solution. Wentzel and Goldberger checked my analysis as I could not quite believe the result myself."

Let us introduce the Alfvén angular velocity [47]

$$\omega_{A_\phi} = \frac{B_\phi^0}{R\sqrt{\rho\mu_0}} \tag{1.4}$$

as well as the hydrodynamic Rossby number

$$\mathrm{Ro} := \frac{R}{2\Omega}\partial_R\Omega \tag{1.5}$$

and the magnetic Rossby number [31]

$$\mathrm{Rb} := \frac{R}{2B_\phi^0 R^{-1}}\partial_R(B_\phi^0 R^{-1}), \tag{1.6}$$

where $\partial_R = \frac{\partial}{\partial R}$. The Chandrasekhar equipartition solution implies that [34, 35]

$$\Omega = \omega_{A_\phi}, \quad \mathrm{Ro} = \mathrm{Rb} = -1. \tag{1.7}$$

The latter equality follows from the condition of the constant total pressure and from the fact that in the steady-state the centrifugal acceleration of the background flow is compensated by the pressure gradient: $R\Omega^2 = \frac{1}{\rho}\partial_R p_0$. Note that $\mathrm{Ro} = -1$ corresponds to the velocity profile $\Omega(R) \sim R^{-2}$ whereas $\mathrm{Rb} = -1$ corresponds to the magnetic field produced by an axial current I isolated from the fluid [35]: $B_\phi^0(R) = \frac{\mu_0 I}{2\pi R}$.

Note that the Chandrasekhar equipartition solution belongs to a wide class of exact steady-state solutions of the equations of ideal magnetohydrodynamics (MHD)—the solutions with constant total pressure—see [7] and [22] for recent achievements in this field.

In the absence of the magnetic field the rotational flow of the ideal fluid is stable with respect to axisymmetric perturbations if and only if $\mathrm{Ro} > -1$ (the Rayleigh criterion [50]). Otherwise, it becomes centrifugally unstable via a steady-state bifurcation [29]. Note that the ideal flow with the Keplerian rotation profile, i.e. with $\Omega(R) \propto R^{-3/2}$, is hydrodynamically stable because $\mathrm{Ro} = -\frac{3}{4} > -1$.

According to the Michael's criterion [45], the rotational flow of the ideal and perfectly conducting fluid subject to the azimuthal magnetic field, is stable with respect to axisymmetric perturbations, if

$$\delta := \mathrm{Ro} - \mathrm{Rb}\mathrm{N}^2 > -1, \tag{1.8}$$

where

$$\mathrm{N} = \frac{\omega_{A_\phi}}{\Omega}. \tag{1.9}$$

Obviously, inequality (1.8) is valid for Chandrasekhar's equipartition solution (1.7).

Nonaxisymmetric instabilities of the rotating flow of inviscid and perfectly conducting fluid were studied in [3], [47], and [64]. In the short-wavelength approximation it was found that in the limit of infinitely large axial and azimuthal wavenumbers of the perturbation, the hydrodynamically stable flow is destabilized by a weak azimuthal magnetic field, if

$$N^2 < -\frac{4\mathrm{Ro}}{n^2}, \tag{1.10}$$

where $n \gg 1$ is the azimuthal wavenumber and $\mathrm{Ro} < 0$. Moreover, in the limit $n \to \infty$ the growth rate of the perturbation tends to the Oort's value $|\Omega \mathrm{Ro}|$ [47]. Therefore, in the case of ideal magnetohydrodynamics, i.e. when $\nu = 0$ and $\eta = 0$, the hydrodynamically stable flows with $-1 < \mathrm{Ro} < 0$, including the Keplerian flow with $\mathrm{Ro} = -\frac{3}{4}$, can suffer from the azimuthal magnetorotational instability (AMRI) when the condition (1.10) is fulfilled. Again, the Chandrasekhar equipartition solution (1.7) violates the instability condition (1.10) already at $n > 2$.

The physical mechanism of non-axisymmetric AMRI in the ideal MHD case is destabilization of slow magneto-Coriolis waves [64], quite similar to the axisymmetric standard magnetorotational instability of Velikhov and Chandrasekhar [2, 13, 60] that takes place in the magnetized rotating flow subject to the axial magnetic field [28, 29].

Both standard and azimuthal magnetorotational instabilities are considered as the most probable candidates to the role of triggers of turbulence in accretion disks, protoplanetary systems and even in stars and planetary interiors [2, 3, 35, 52, 53]. Standard magnetorotational instability is relative to the instabilities arising in the artificial space tethered systems, such as couples of tethered satellites or even rings of connected satellites orbiting a planet [2, 4, 41]. On the other hand, the azimuthal magnetorotational instability has an analog in viscoelastic instability in rotating polymer flows in the limit of infinite relaxation time of the complex fluid [48, 49]. Both analogies are possible because the magnetic field lines that are frozen into the perfectly conducting fluid by the Alfvén theorem 'reinforce' the fluid and make it effectively a complex or non-Newtonian fluid [14]. The analogies not only allow one to understand better the instability mechanism existing in seemingly non-related applications but also open a way to study magnetohydrodynamical instabilities in the compact laboratory experiments with polymer fluids [8].

Realistic modeling of astrophysical phenomena where magnetorotational instabilities play a crucial part requires taking into account dissipative effects of different physical nature [46]. Although the particular dissipative mechanisms can be rather weak, their relative strengths may differ by orders of magnitude. The latter circumstance makes numerical computations expensive because of the necessity to deal with multiple scales and to resolve fine structures. By this reason laboratory experiments with electrically conducting media, such as liquid metals or plasmas, in magnetic fields are being developed worldwide in order to supplement the numerical and theoretical studies of magnetorotational instabilities [17, 23, 57].

At the moment, an evidence of helical and azimuthal magnetorotational instability was demonstrated in the laboratory experiments with the Couette-Taylor flow of a liquid metal with specific velocity profiles in the helical (i.e. axial plus azimuthal) or pure azimuthal magnetic field [51, 54]. Liquid metals are materials characterized by a very small ratio of viscosity of the fluid to its electrical resistivity. The ratio, which is called the magnetic Prandtl number $\left(\mathrm{Pm} = \frac{\nu}{\eta}\right)$ is typically of order $10^{-6} - 10^{-5}$ in these materials. By this reason, the onset of the standard magnetorotational instability requires very high rotation speeds of the cylinders of the Couette-Taylor cell that make sustaining the laminar flow in the absence of the magnetic field problematic [23]. The same material property of the liquid metals prevents destabilization of Keplerian flows in the successful experiments with the azimuthal or helical magnetic fields where the azimuthal component is created by an isolated from the fluid axial current [23]. Indeed, at $\mathrm{Rb} = -1$ the range of hydrodynamically stable flows that are susceptible to destabilization by the azimuthal or helical magnetic field is limited by the Rossby numbers from $\mathrm{Ro} = -1$ to $\mathrm{Ro} = 2 - 2\sqrt{2}$, which does not contain the Keplerian profile with $\mathrm{Ro} = -\frac{3}{4}$ [30, 42]. Therefore, the existing liquid metal experiments require further improvements in order to be able modeling the astrophysically relevant instabilities in the lab [23].

Recent letter [31] demonstrated a possibility to destabilize a hydrodynamically stable Couette-Taylor flow of a liquid metal in the case when the constraint $\mathrm{Rb} = -1$ is relaxed. Physically this can happen due to the contribution to the azimuthal field from the electrical currents through the liquid metal in addition to the field created by an isolated axial current [34, 35]. A remarkably simple instability condition was found in [31] that relates the hydrodynamic and magnetic Rossby numbers in the limit of vanishing Pm:

$$\mathrm{Rb} > -\frac{1}{8}\frac{(\mathrm{Ro}+2)^2}{\mathrm{Ro}+1}, \tag{1.11}$$

which implies destabilization of the Keplerian flow when $\mathrm{Rb} > \mathrm{Rb}^{crit} = -\frac{25}{32}$, i.e. when the radial profile of the azimuthal field is slightly flatter than R^{-1}. Note how dramatically different are conditions for destabilization of a Keplerian flow by the azimuthal magnetic field in the case of ideal MHD when non-axisymmetric instability can happen already at $\mathrm{Rb} = -1$ and in the viscous and resistive case with $\mathrm{Pm} \ll 1$ when there exists a critical steepness $\mathrm{Rb}^{crit} > -1$ for the radial profile of the magnetic field.

The discrepancy between the stability thresholds of an ideal system without dissipation and that of the system with the dissipation included in the limit when the dissipation tends to zero is a universal phenomenon that is known in many areas of physics and engineering for decades [27]. In plasma physics and magnetohydrodynamics it has already lead to rather radical conclusions [46]: "A great deal of time was wasted analyzing ideal MHD equilibria which could never be reached as the limit of a resistive equilibrium with small but non-zero resistivity. The result has been an imprecision in the conceptualizations which is likely to be very difficult to sharpen up. It is perhaps the reason that theory is taken more as a decoration to experiments, at the present time, than as a guide to where to go next with them." The same phenomenon is known in hydrodynamics, e.g. for the baroclinic instability [37, 58], Benjamin-Feir modulational instability [11, 32] and instability of a stably stratified shear flow [59]. In mechanical engineering this effect is known since 1952 as the Ziegler paradox [63], where it was recognized as the problem of the "greatest theoretical interest" [9].

In 1956 Bottema [10, 27] discovered a link between the Ziegler paradox and the singularity "Whitney umbrella" on the boundary of the asymptotic stability domain of a dissipative system. After the 1971 work by Arnold [1] on generic singularities in the multiparameter families of matrices the researchers in applications gradually accepted this point of view and developed methods of investigation of the destabilization paradox and dissipation-induced instabilities in systems with multiple damping mechanisms via perturbation of multiple eigenvalues, index theory and exploitation of the fundamental symmetries of the ideal system [6, 26, 27, 33, 40, 43, 44]. Note that the role of mutual strengths of different dissipation mechanisms on stability thresholds was emphasized already in the works by Smith [55] and Kapitsa [24] on rotor dynamics in the 1930s.

In a recent work [35] first indications were obtained that the azimuthal magnetorotational instability can be caused by a dissipative perturbation of the Chandrasekhar equipartition solution of ideal MHD. In the present paper we pursue this idea further by re-deriving the WKB equations of the problem, writing the corresponding algebraic eigenvalue problem, which determines the dispersion relation of the ideal system, in the Hamiltonian form and then studying systematically its non-Hamiltonian perturbation by the viscous and resistive terms. We find the conditions when the azimuthal MRI is indeed a dissipation-induced instability of the Chandrasekhar equipartition solution or its extensions.

2. Geometrical optics equations

Linearizing equations (1.1)-(1.2) in the vicinity of the stationary solution (1.3) by assuming general perturbations $\boldsymbol{u} = \boldsymbol{u}_0 + \boldsymbol{u}'$, $p = p_0 + p'$, and $\boldsymbol{B} = \boldsymbol{B}_0 + \boldsymbol{B}'$ and leaving only the terms of first order with respect to the primed quantities, we find [35, 38]:

$$\begin{gathered}\partial_t \boldsymbol{u}' + \boldsymbol{u}_0 \cdot \boldsymbol{\nabla} \boldsymbol{u}' + \boldsymbol{u}' \cdot \boldsymbol{\nabla} \boldsymbol{u}_0 - \frac{1}{\rho\mu_0}\left(\boldsymbol{B}_0 \cdot \boldsymbol{\nabla} \boldsymbol{B}' + \boldsymbol{B}' \cdot \boldsymbol{\nabla} \boldsymbol{B}_0\right) - \nu \boldsymbol{\nabla}^2 \boldsymbol{u}' = \\ -\frac{1}{\rho}\boldsymbol{\nabla} p' - \frac{1}{\rho\mu_0}\boldsymbol{\nabla}(\boldsymbol{B}_0 \cdot \boldsymbol{B}'), \\ \partial_t \boldsymbol{B}' + \boldsymbol{u}_0 \cdot \boldsymbol{\nabla} \boldsymbol{B}' + \boldsymbol{u}' \cdot \boldsymbol{\nabla} \boldsymbol{B}_0 - \boldsymbol{B}_0 \cdot \boldsymbol{\nabla} \boldsymbol{u}' - \boldsymbol{B}' \cdot \boldsymbol{\nabla} \boldsymbol{u}_0 - \eta \boldsymbol{\nabla}^2 \boldsymbol{B}' = 0, \end{gathered} \tag{2.1}$$

where the perturbations fulfil the constraints

$$\boldsymbol{\nabla} \cdot \boldsymbol{u}' = 0, \quad \boldsymbol{\nabla} \cdot \boldsymbol{B}' = 0. \tag{2.2}$$

Introducing the gradients of the background fields represented by the two 3×3 matrices

$$\mathcal{U}(R) = \boldsymbol{\nabla} \boldsymbol{u}_0 = \Omega \begin{pmatrix} 0 & -1 & 0 \\ 1 + 2\mathrm{Ro} & 0 & 0 \\ 0 & 0 & 0 \end{pmatrix}, \quad \mathcal{B}(R) = \boldsymbol{\nabla} \boldsymbol{B}_0 = \frac{B_\phi^0}{R} \begin{pmatrix} 0 & -1 & 0 \\ 1 + 2\mathrm{Rb} & 0 & 0 \\ 0 & 0 & 0 \end{pmatrix}, \tag{2.3}$$

we write the linearized system of magnetohydrodynamics in the form [35]

$$\left(\begin{array}{cc} \partial_t+\mathcal{U}+\boldsymbol{u}_0\cdot\boldsymbol{\nabla}-\nu\boldsymbol{\nabla}^2 & -\frac{1}{\rho\mu_0}\left(\mathcal{B}+\boldsymbol{B}_0\cdot\boldsymbol{\nabla}\right) \\ \mathcal{B}-\boldsymbol{B}_0\cdot\boldsymbol{\nabla} & \partial_t-\mathcal{U}+\boldsymbol{u}_0\cdot\boldsymbol{\nabla}-\eta\boldsymbol{\nabla}^2 \end{array}\right)\left(\begin{array}{c} \boldsymbol{u}' \\ \boldsymbol{B}' \end{array}\right)+\frac{\boldsymbol{\nabla}}{\rho}\left(\begin{array}{c} p'+\frac{1}{\mu_0}(\boldsymbol{B}_0\cdot\boldsymbol{B}') \\ 0 \end{array}\right)=0. \quad (2.4)$$

We seek for solutions of the linearized equations (2.4) in the form of the 'geometrical optics' asymptotic series with respect to the small parameter ϵ, $0<\epsilon\ll 1$ [33]:

$$\begin{aligned} \boldsymbol{u}'(\boldsymbol{x},t,\epsilon) &= e^{i\Phi(\boldsymbol{x},t)/\epsilon}\left(\boldsymbol{u}^{(0)}(\boldsymbol{x},t)+\epsilon\boldsymbol{u}^{(1)}(\boldsymbol{x},t)\right)+\epsilon\boldsymbol{u}^{(r)}(\boldsymbol{x},t), \\ \boldsymbol{B}'(\boldsymbol{x},t,\epsilon) &= e^{i\Phi(\boldsymbol{x},t)/\epsilon}\left(\boldsymbol{B}^{(0)}(\boldsymbol{x},t)+\epsilon\boldsymbol{B}^{(1)}(\boldsymbol{x},t)\right)+\epsilon\boldsymbol{B}^{(r)}(\boldsymbol{x},t), \\ p'(\boldsymbol{x},t,\epsilon) &= e^{i\Phi(\boldsymbol{x},t)/\epsilon}\left(p^{(0)}(\boldsymbol{x},t)+\epsilon p^{(1)}(\boldsymbol{x},t)\right)+\epsilon p^{(r)}(\boldsymbol{x},t), \end{aligned} \quad (2.5)$$

where $\boldsymbol{x}$ is a vector of coordinates, Φ is a real-valued scalar function that represents the phase of oscillations, and $\boldsymbol{u}^{(j)}$, $\boldsymbol{B}^{(j)}$, and $p^{(j)}$, $j=0,1,r$ are complex-valued amplitudes with the index r denoting residual terms.

Following [16, 18, 39] we assume that $\nu=\epsilon^2\tilde{\nu}$ and $\eta=\epsilon^2\tilde{\eta}$. Substituting expansions (2.5) in (2.4) and collecting terms at ϵ^{-1} and ϵ^0, we arrive at the two systems of equations [35]

$$\left(\begin{array}{cc} \partial_t\Phi+(\boldsymbol{u}_0\cdot\boldsymbol{\nabla}\Phi) & -\frac{1}{\rho\mu_0}(\boldsymbol{B}_0\cdot\boldsymbol{\nabla}\Phi) \\ -(\boldsymbol{B}_0\cdot\boldsymbol{\nabla}\Phi) & \partial_t\Phi+(\boldsymbol{u}_0\cdot\boldsymbol{\nabla}\Phi) \end{array}\right)\left(\begin{array}{c} \boldsymbol{u}^{(0)} \\ \boldsymbol{B}^{(0)} \end{array}\right)=-\frac{\boldsymbol{\nabla}\Phi}{\rho}\left(\begin{array}{c} p^{(0)}+\frac{1}{\mu_0}(\boldsymbol{B}_0\cdot\boldsymbol{B}^{(0)}) \\ 0 \end{array}\right), \quad (2.6)$$

$$\begin{aligned} & i\left(\begin{array}{cc} \partial_t\Phi+(\boldsymbol{u}_0\cdot\boldsymbol{\nabla}\Phi) & -\frac{1}{\rho\mu_0}(\boldsymbol{B}_0\cdot\boldsymbol{\nabla}\Phi) \\ -(\boldsymbol{B}_0\cdot\boldsymbol{\nabla}\Phi) & \partial_t\Phi+(\boldsymbol{u}_0\cdot\boldsymbol{\nabla}\Phi) \end{array}\right)\left(\begin{array}{c} \boldsymbol{u}^{(1)} \\ \boldsymbol{B}^{(1)} \end{array}\right)+i\frac{\boldsymbol{\nabla}\Phi}{\rho}\left(\begin{array}{c} p^{(1)}+\frac{1}{\mu_0}(\boldsymbol{B}_0\cdot\boldsymbol{B}^{(1)}) \\ 0 \end{array}\right) \\ & +\left(\begin{array}{cc} \partial_t+\mathcal{U}+\boldsymbol{u}_0\cdot\boldsymbol{\nabla}+\tilde{\nu}(\boldsymbol{\nabla}\Phi)^2 & -\frac{1}{\rho\mu_0}\left(\mathcal{B}+\boldsymbol{B}_0\cdot\boldsymbol{\nabla}\right) \\ \mathcal{B}-\boldsymbol{B}_0\cdot\boldsymbol{\nabla} & \partial_t-\mathcal{U}+\boldsymbol{u}_0\cdot\boldsymbol{\nabla}+\tilde{\eta}(\boldsymbol{\nabla}\Phi)^2 \end{array}\right)\left(\begin{array}{c} \boldsymbol{u}^{(0)} \\ \boldsymbol{B}^{(0)} \end{array}\right) \\ & +\frac{\boldsymbol{\nabla}}{\rho}\left(\begin{array}{c} p^{(0)}+\frac{1}{\mu_0}(\boldsymbol{B}_0\cdot\boldsymbol{B}^{(0)}) \\ 0 \end{array}\right)=0. \end{aligned} \quad (2.7)$$

From the solenoidality conditions (2.2) it follows that

$$\begin{aligned} \boldsymbol{u}^{(0)}\cdot\boldsymbol{\nabla}\Phi=0, &\quad \boldsymbol{\nabla}\cdot\boldsymbol{u}^{(0)}+i\boldsymbol{u}^{(1)}\cdot\boldsymbol{\nabla}\Phi=0, \\ \boldsymbol{B}^{(0)}\cdot\boldsymbol{\nabla}\Phi=0, &\quad \boldsymbol{\nabla}\cdot\boldsymbol{B}^{(0)}+i\boldsymbol{B}^{(1)}\cdot\boldsymbol{\nabla}\Phi=0. \end{aligned} \quad (2.8)$$

The dot product of the first of the equations in the system (2.6) with $\boldsymbol{\nabla}\Phi$ under the constraints (2.8) yields

$$(\nabla\Phi)^2\left(\frac{p^{(0)}}{\rho}+\frac{1}{\rho\mu_0}(\boldsymbol{B}_0\cdot\boldsymbol{B}^{(0)})\right)=0. \quad (2.9)$$

Consequently, if $\boldsymbol{\nabla}\Phi\neq 0$, then

$$p^{(0)}=-\frac{1}{\mu_0}(\boldsymbol{B}_0\cdot\boldsymbol{B}^{(0)}). \quad (2.10)$$

Under the condition (2.10) the equation (2.6) has a nontrivial solution if the determinant of the 6×6 matrix in its left-hand side is vanishing. This gives us two characteristic roots corresponding to the two Alfvén waves [19, 20, 38] that originate the following two Hamilton-Jacobi equations for the phase Φ:

$$\partial_t\Phi+\left(\boldsymbol{u}_0\pm\frac{\boldsymbol{B}_0}{\sqrt{\rho\mu_0}}\right)\cdot\boldsymbol{\nabla}\Phi=0. \quad (2.11)$$

The characteristic roots $\left(-\boldsymbol{u}_0 \pm \frac{\boldsymbol{B}_0}{\sqrt{\rho\mu_0}}\right)\cdot\boldsymbol{\nabla}\Phi$ are triple and semi-simple with the eigenvectors

$$\begin{pmatrix} 0 \\ 0 \\ \frac{\pm 1}{\sqrt{\rho\mu_0}} \\ 0 \\ 0 \\ 1 \end{pmatrix}, \quad \begin{pmatrix} 0 \\ \frac{\pm 1}{\sqrt{\rho\mu_0}} \\ 0 \\ 0 \\ 1 \\ 0 \end{pmatrix}, \quad \begin{pmatrix} \frac{\pm 1}{\sqrt{\rho\mu_0}} \\ 0 \\ 0 \\ 1 \\ 0 \\ 0 \end{pmatrix}. \tag{2.12}$$

On the surface

$$\boldsymbol{B}_0\cdot\boldsymbol{\nabla}\Phi = 0 \tag{2.13}$$

the triple Alfvén roots merge into a semi-simple characteristic root of multiplicity 6 [19, 20, 38]. Then,

$$\frac{D\Phi}{Dt} = 0, \tag{2.14}$$

where $\frac{D}{Dt} := \partial_t + \boldsymbol{u}_0\cdot\boldsymbol{\nabla}$ is the derivative along the fluid stream lines. Taking the gradient of (2.14) yields

$$\begin{aligned}\boldsymbol{\nabla}\partial_t\Phi + \boldsymbol{\nabla}(\boldsymbol{u}_0\cdot\boldsymbol{\nabla})\Phi &= \partial_t\boldsymbol{\nabla}\Phi + (\boldsymbol{u}_0\cdot\boldsymbol{\nabla})\boldsymbol{\nabla}\Phi + \mathcal{U}^T\boldsymbol{\nabla}\Phi \\ &= \tfrac{D}{Dt}\boldsymbol{\nabla}\Phi + \mathcal{U}^T\boldsymbol{\nabla}\Phi = 0.\end{aligned} \tag{2.15}$$

Similarly,

$$\boldsymbol{\nabla}(\boldsymbol{B}_0\cdot\boldsymbol{\nabla}\Phi) = (\boldsymbol{B}_0\cdot\boldsymbol{\nabla})\boldsymbol{\nabla}\Phi + \mathcal{B}^T\boldsymbol{\nabla}\Phi = 0. \tag{2.16}$$

With the use of the relations (2.10), (2.13), (2.14) we simplify the equations (2.7) as

$$\begin{aligned}\left(\tfrac{D}{Dt} + \tilde{\nu}(\boldsymbol{\nabla}\Phi)^2 + \mathcal{U}\right)\boldsymbol{u}^{(0)} - \tfrac{1}{\rho\mu_0}(\mathcal{B} + \boldsymbol{B}_0\cdot\boldsymbol{\nabla})\boldsymbol{B}^{(0)} &= -\tfrac{i}{\rho}\left(p^{(1)} + \tfrac{1}{\mu_0}(\boldsymbol{B}_0\cdot\boldsymbol{B}^{(1)})\right)\boldsymbol{\nabla}\Phi, \\ \left(\tfrac{D}{Dt} + \tilde{\eta}(\boldsymbol{\nabla}\Phi)^2 - \mathcal{U}\right)\boldsymbol{B}^{(0)} + (\mathcal{B} - \boldsymbol{B}_0\cdot\boldsymbol{\nabla})\boldsymbol{u}^{(0)} &= 0.\end{aligned} \tag{2.17}$$

Eliminating pressure in the first of Eqs. (2.17) via multiplication of it by $\boldsymbol{\nabla}\Phi$ and taking into account the constraints (2.8), we transform this equation into

$$\begin{aligned}&\left(\tfrac{D}{Dt} + \tilde{\nu}(\boldsymbol{\nabla}\Phi)^2 + \mathcal{U}\right)\boldsymbol{u}^{(0)} - \tfrac{1}{\rho\mu_0}(\mathcal{B} + \boldsymbol{B}_0\cdot\boldsymbol{\nabla})\boldsymbol{B}^{(0)} \\ &= \tfrac{\boldsymbol{\nabla}\Phi}{|\boldsymbol{\nabla}\Phi|^2}\cdot\left[\left(\tfrac{D}{Dt} + \mathcal{U}\right)\boldsymbol{u}^{(0)} - \tfrac{1}{\rho\mu_0}(\mathcal{B} + \boldsymbol{B}_0\cdot\boldsymbol{\nabla})\boldsymbol{B}^{(0)}\right]\boldsymbol{\nabla}\Phi,\end{aligned} \tag{2.18}$$

in accordance with the standard procedure described, e.g., in [61]. Differentiating the first of the identities (2.8) yields

$$\frac{D}{Dt}(\boldsymbol{\nabla}\Phi\cdot\boldsymbol{u}^{(0)}) = \frac{D\boldsymbol{\nabla}\Phi}{Dt}\cdot\boldsymbol{u}^{(0)} + \boldsymbol{\nabla}\Phi\cdot\frac{D\boldsymbol{u}^{(0)}}{Dt} = 0. \tag{2.19}$$

On the other hand, from the third of the identities (2.8) it follows that

$$(\boldsymbol{B}_0\cdot\boldsymbol{\nabla})(\boldsymbol{\nabla}\Phi\cdot\boldsymbol{B}^{(0)}) = ((\boldsymbol{B}_0\cdot\boldsymbol{\nabla})\boldsymbol{\nabla}\Phi)\cdot\boldsymbol{B}^{(0)} + \boldsymbol{\nabla}\Phi\cdot(\boldsymbol{B}_0\cdot\boldsymbol{\nabla})\boldsymbol{B}^{(0)} = 0. \tag{2.20}$$

Using the identities (2.19) and (2.20), we re-write Eq. (2.18) as follows

$$\begin{aligned}&\left(\tfrac{D}{Dt} + \tilde{\nu}(\boldsymbol{\nabla}\Phi)^2 + \mathcal{U}\right)\boldsymbol{u}^{(0)} - \tfrac{1}{\rho\mu_0}(\mathcal{B} + \boldsymbol{B}_0\cdot\boldsymbol{\nabla})\boldsymbol{B}^{(0)} \\ &= \tfrac{\boldsymbol{\nabla}\Phi}{|\boldsymbol{\nabla}\Phi|^2}\cdot\left[\mathcal{U}\boldsymbol{u}^{(0)} - \tfrac{1}{\rho\mu_0}\mathcal{B}\boldsymbol{B}^{(0)}\right]\boldsymbol{\nabla}\Phi + \tfrac{1}{\rho\mu_0}\tfrac{\boldsymbol{\nabla}\Phi}{|\boldsymbol{\nabla}\Phi|^2}((\boldsymbol{B}_0\cdot\boldsymbol{\nabla})\boldsymbol{\nabla}\Phi)\cdot\boldsymbol{B}^{(0)} - \tfrac{\boldsymbol{\nabla}\Phi}{|\boldsymbol{\nabla}\Phi|^2}\tfrac{D\boldsymbol{\nabla}\Phi}{Dt}\cdot\boldsymbol{u}^{(0)}.\end{aligned} \tag{2.21}$$

With the identities (2.16) and (2.15) the equation (2.21) and, consequently, the first of the equations (2.17) transforms into

$$\begin{aligned}&\left(\tfrac{D}{Dt} + \tilde{\nu}(\boldsymbol{\nabla}\Phi)^2 + \mathcal{U}\right)\boldsymbol{u}^{(0)} - \tfrac{1}{\rho\mu_0}(\mathcal{B} + \boldsymbol{B}_0\cdot\boldsymbol{\nabla})\boldsymbol{B}^{(0)} \\ &= \boldsymbol{\nabla}\Phi\tfrac{\boldsymbol{\nabla}\Phi}{|\boldsymbol{\nabla}\Phi|^2}\cdot\left[\mathcal{U}\boldsymbol{u}^{(0)} - \tfrac{1}{\rho\mu_0}\mathcal{B}\boldsymbol{B}^{(0)}\right] - \tfrac{1}{\rho\mu_0}\tfrac{\boldsymbol{\nabla}\Phi}{|\boldsymbol{\nabla}\Phi|^2}\mathcal{B}^T\boldsymbol{\nabla}\Phi\cdot\boldsymbol{B}^{(0)} + \tfrac{\boldsymbol{\nabla}\Phi}{|\boldsymbol{\nabla}\Phi|^2}\mathcal{U}^T\boldsymbol{\nabla}\Phi\cdot\boldsymbol{u}^{(0)} \\ &= 2\tfrac{\boldsymbol{\nabla}\Phi(\boldsymbol{\nabla}\Phi)^T}{|\boldsymbol{\nabla}\Phi|^2}\left[\mathcal{U}\boldsymbol{u}^{(0)} - \tfrac{1}{\rho\mu_0}\mathcal{B}\boldsymbol{B}^{(0)}\right].\end{aligned} \tag{2.22}$$

Denoting $\boldsymbol{k} = \boldsymbol{\nabla}\Phi$, we deduce from the phase equation (2.15) that

$$\frac{D\boldsymbol{k}}{Dt} = -\mathcal{U}^T\boldsymbol{k}. \tag{2.23}$$

Similarly, the transport equations for the amplitudes (2.17) take the final form

$$\begin{aligned} \frac{D\boldsymbol{u}^{(0)}}{Dt} &= -\left(\mathcal{I} - \frac{2\boldsymbol{k}\boldsymbol{k}^T}{|\boldsymbol{k}|^2}\right)\mathcal{U}\boldsymbol{u}^{(0)} - \tilde{\nu}|\boldsymbol{k}|^2\boldsymbol{u}^{(0)} + \frac{1}{\rho\mu_0}\left(\left(\mathcal{I} - \frac{2\boldsymbol{k}\boldsymbol{k}^T}{|\boldsymbol{k}|^2}\right)\mathcal{B} + \boldsymbol{B}_0\cdot\boldsymbol{\nabla}\right)\boldsymbol{B}^{(0)}, \\ \frac{D\boldsymbol{B}^{(0)}}{Dt} &= \mathcal{U}\boldsymbol{B}^{(0)} - \tilde{\eta}|\boldsymbol{k}|^2\boldsymbol{B}^{(0)} - (\mathcal{B} - \boldsymbol{B}_0\cdot\boldsymbol{\nabla})\boldsymbol{u}^{(0)}. \end{aligned} \tag{2.24}$$

where $\mathcal{I}$ is a 3×3 identity matrix. Recall that the equations (2.23) and (2.24) are valid under the assumption that the condition (2.13) is fulfilled.

The local partial differential equations (2.24) are equivalent to the transport equations derived in [33–35]. In case of ideal MHD when viscosity and resistivity are zero, the equations (2.24) exactly coincide with those of the work [38] and are equivalent to the transport equations derived in [21, 61]. In the absence of the magnetic field these equations can be treated as ordinary differential equations with respect to the convective derivative $\frac{D}{Dt}$ and thus are reduced to that of the work [18] that considered stability of the viscous Couette-Taylor flow. Note that the same form of the amplitude equations (with the different matrix $\mathcal{U}$) appears in the studies of elliptical instability in [39] and of three-dimensional local instabilities of more general viscous and inviscid basic flows in [16].

3. Dispersion relation of the amplitude equations

Let the orthogonal unit vectors $\boldsymbol{e}_R(t)$, $\boldsymbol{e}_\phi(t)$, and $\boldsymbol{e}_z(t)$ form a basis in a cylindrical coordinate system moving along the fluid trajectory. With $\boldsymbol{k}(t) = k_R\boldsymbol{e}_R(t) + k_\phi\boldsymbol{e}_\phi(t) + k_z\boldsymbol{e}_z(t)$, $\boldsymbol{u}(t) = u_R\boldsymbol{e}_R(t) + u_\phi\boldsymbol{e}_\phi(t) + u_z\boldsymbol{e}_z(t)$, and with the matrix $\mathcal{U}$ from (2.3), we find

$$\dot{\boldsymbol{e}}_R = \Omega(R)\mathbf{e}_\phi, \quad \dot{\boldsymbol{e}}_\phi = -\Omega(R)\boldsymbol{e}_R. \tag{3.1}$$

Hence, the equation (2.23) in the coordinate form is

$$\dot{k}_R = -R\partial_R\Omega k_\phi, \quad \dot{k}_\phi = 0, \quad \dot{k}_z = 0. \tag{3.2}$$

According to [18] and [21], in order to study physically relevant and potentially unstable modes we have to choose bounded and asymptotically non-decaying solutions of the system (3.2). These correspond to $k_\phi \equiv 0$ and k_R and k_z time-independent. Note that this solution is compatible with the constraint $\boldsymbol{B}_0\cdot\boldsymbol{k} = 0$ following from (2.13).

Denoting $\alpha = k_z|\boldsymbol{k}|^{-1}$, where $|\boldsymbol{k}|^2 = k_R^2 + k_z^2$, and find that $k_R k_z^{-1} = \sqrt{1-\alpha^2}\alpha^{-1}$ we write the local partial differential equations (2.24) for the amplitudes in the coordinate representation. Then, the equations for the axial components are separated from the equations for the radial and azimuthal components. The latter are as follows [34, 35]:

$$\begin{gathered} \left(\partial_t + \Omega\partial_\phi + \widetilde{\nu}|\boldsymbol{k}|^2\right)u_R^{(0)} - 2\alpha^2\Omega u_\phi^{(0)} - \tfrac{B_\phi^0}{\rho\mu_0 R}\partial_\phi B_R^{(0)} + 2\alpha^2\tfrac{B_\phi^0}{\rho\mu_0 R}B_\phi^{(0)} = 0, \\ \left(\partial_t + \Omega\partial_\phi + \widetilde{\nu}|\boldsymbol{k}|^2\right)u_\phi^{(0)} + 2\Omega(1+\mathrm{Ro})u_R^{(0)} - \tfrac{2}{\rho\mu_0}\tfrac{B_\phi^0}{R}(1+\mathrm{Rb})B_R^{(0)} - \tfrac{1}{\rho\mu_0}\tfrac{B_\phi^0}{R}\partial_\phi B_\phi^{(0)} = 0, \\ \left(\partial_t + \Omega\partial_\phi + \widetilde{\eta}|\boldsymbol{k}|^2\right)B_R^{(0)} - \tfrac{B_\phi^0}{R}\partial_\phi u_R^{(0)} = 0, \\ \left(\partial_t + \Omega\partial_\phi + \widetilde{\eta}|\boldsymbol{k}|^2\right)B_\phi^{(0)} - 2\Omega\mathrm{Ro}B_R^{(0)} + 2\mathrm{Rb}\tfrac{B_\phi^0}{R}u_R^{(0)} - \tfrac{B_\phi^0}{R}\partial_\phi u_\phi^{(0)} = 0. \end{gathered} \tag{3.3}$$

We look for a solution to Eqs. (3.3) in the modal form: $\boldsymbol{u}^{(0)} = \widehat{\boldsymbol{u}} e^{\alpha\Omega\lambda t + im\phi}$, $\boldsymbol{B}^{(0)} = \sqrt{\rho\mu_0}\widehat{\boldsymbol{B}} e^{\alpha\Omega\lambda t + im\phi}$ and introduce the viscous and resistive frequencies, the modified azimuthal wavenumber, and the hydrodynamic and magnetic Reynolds numbers [34, 35]:

$$\omega_\nu = \widetilde{\nu}|\boldsymbol{k}|^2, \quad \omega_\eta = \widetilde{\eta}|\boldsymbol{k}|^2, \quad n = \frac{m}{\alpha}, \quad \mathrm{Re} = \frac{\alpha\Omega}{\omega_\nu}, \quad \mathrm{Rm} = \frac{\alpha\Omega}{\omega_\eta}. \tag{3.4}$$

We write the amplitude equations (3.3) in the matrix form

$$\mathbf{A}\mathbf{z} = \lambda\mathbf{z}, \tag{3.5}$$

where $\mathbf{z} = (\widehat{u}_R, \widehat{u}_\phi, \widehat{B}_R, \widehat{B}_\phi)^T$ and $\mathbf{A} = \mathbf{A}_0 + \mathbf{A}_1$ with [31, 34, 35, 56]

$$\mathbf{A}_0 = \begin{pmatrix} -in & 2\alpha & in\mathrm{N} & -2\alpha\mathrm{N} \\ -\frac{2(1+\mathrm{Ro})}{\alpha} & -in & \frac{2(1+\mathrm{Rb})}{\alpha}\mathrm{N} & in\mathrm{N} \\ in\mathrm{N} & 0 & -in & 0 \\ -\frac{2\mathrm{Rb}}{\alpha}\mathrm{N} & in\mathrm{N} & \frac{2\mathrm{Ro}}{\alpha} & -in \end{pmatrix}, \quad \mathbf{A}_1 = -\begin{pmatrix} \frac{1}{\mathrm{Re}} & 0 & 0 & 0 \\ 0 & \frac{1}{\mathrm{Re}} & 0 & 0 \\ 0 & 0 & \frac{1}{\mathrm{Rm}} & 0 \\ 0 & 0 & 0 & \frac{1}{\mathrm{Rm}} \end{pmatrix}. \tag{3.6}$$

The solvability condition written for the above system of algebraic equations yields the dispersion relation

$$p(\lambda) := \det(\mathbf{A} - \lambda\mathbf{I}) = 0, \tag{3.7}$$

where $\mathbf{I}$ is the 4×4 identity matrix, and $p(\lambda)$ is a complex fourth-order polynomial

$$p(\lambda) = (a_0 + ib_0)\lambda^4 + (a_1 + ib_1)\lambda^3 + (a_2 + ib_2)\lambda^2 + (a_3 + ib_3)\lambda + a_4 + ib_4. \tag{3.8}$$

In the particular case when $\omega_\nu = 0$, $\omega_\eta = 0$ the coefficients of the dispersion relation (3.7) exactly coincide with those derived in the works [21, 47]. In the absence of the magnetic field, the dispersion relation (3.7) reduces to that derived in the narrow-gap approximation in [36] for the nonaxisymmetric perturbations of the hydrodynamic Couette-Taylor flow.

4. Hamiltonian formulation

The matrix $\mathbf{A}_0$ in (3.6) corresponds to the ideal system whereas $\mathbf{A}_1$ is its perturbation by the viscous and resistive terms. We would like to reformulate the eigenvalue problem for the matrix $\mathbf{A} = \mathbf{A}_0 + \mathbf{A}_1$ as a problem on the spectrum of Hamiltonian system under a dissipative perturbation [44].

Let us first introduce a Hermitian matrix

$$\mathbf{G} = \begin{pmatrix} 0 & -i & 0 & i\mathrm{N} \\ i & 0 & -i\mathrm{N} & 0 \\ 0 & i\mathrm{N} & 4\frac{\mathrm{Ro}-\mathrm{Rb}}{\alpha n} & -i \\ -i\mathrm{N} & 0 & i & 0 \end{pmatrix}. \tag{4.1}$$

Then, the matrix $\mathbf{H}_0 = -i\mathbf{G}\mathbf{A}_0$ is Hermitian too. Indeed,

$$\mathbf{H}_0 = \begin{pmatrix} -\frac{2(\mathrm{N}^2\mathrm{Rb}-\mathrm{Ro}-1)}{\alpha} & in(\mathrm{N}^2+1) & -\frac{2\mathrm{N}(1+\mathrm{Rb}-\mathrm{Ro})}{\alpha} & -2in\mathrm{N} \\ -in(\mathrm{N}^2+1) & 2\alpha & 2in\mathrm{N} & -2\alpha\mathrm{N} \\ -\frac{2\mathrm{N}(1+\mathrm{Rb}-\mathrm{Ro})}{\alpha} & -2in\mathrm{N} & \frac{2(\mathrm{N}^2\mathrm{Rb}+\mathrm{N}^2+2\mathrm{Rb}-3\mathrm{Ro})}{\alpha} & in(\mathrm{N}^2+1) \\ 2in\mathrm{N} & -2\alpha\mathrm{N} & -in(\mathrm{N}^2+1) & 2\alpha\mathrm{N}^2 \end{pmatrix}. \tag{4.2}$$

Consequently, the eigenvalue problem

$$\mathbf{A}_0\mathbf{z} = \lambda\mathbf{z}$$

can be written in the Hamiltonian form with the Hamiltonian $\mathbf{H}_0$ [33, 62]:

$$\mathbf{H}_0\mathbf{z} = i^{-1}\mathbf{G}\lambda\mathbf{z}. \tag{4.3}$$

The fundamental symmetry

$$\mathbf{A}_0 = -\mathbf{G}^{-1}\overline{\mathbf{A}_0}^T\mathbf{G}, \tag{4.4}$$

where the overbar denotes complex conjugation, implies the symmetry of the spectrum of the matrix $\mathbf{A}_0$ with respect to the imaginary axis [33, 62].

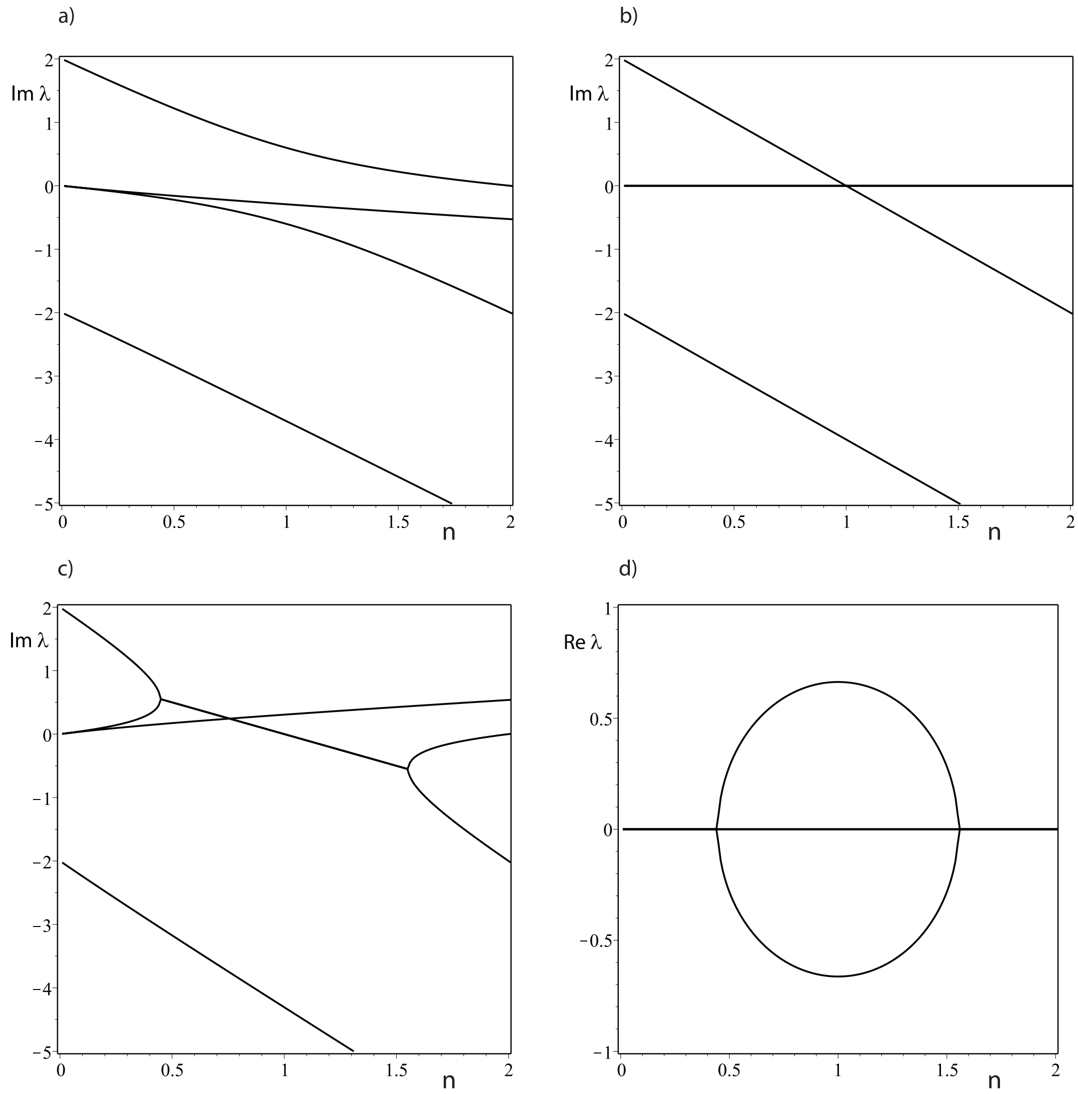

Fig. 1. Frequencies and growth rates of the roots (5.3) and (5.4) of the dispersion relation (5.2) under the constraint $\mathrm{Ro} = \mathrm{RbN}^2$ when (a) $\mathrm{N} = 0.8$, (b) $\mathrm{N} = 1$, and (c,d) $\mathrm{N} = 1.2$.

The full eigenvalue problem (3.5) is thus a dissipative perturbation of the Hamiltonian eigenvalue problem (4.3)

$$(\mathbf{H}_0 + \mathbf{H}_1)\mathbf{z} = i^{-1}\mathbf{G}\lambda\mathbf{z}, \tag{4.5}$$

where $\mathbf{H}_1 = -i\mathbf{G}\mathbf{A}_1$ is a complex non-Hermitian matrix

$$\mathbf{H}_1 = \begin{pmatrix} 0 & \frac{1}{\mathrm{Re}} & 0 & -\frac{\mathrm{N}}{\mathrm{Rm}} \\ -\frac{1}{\mathrm{Re}} & 0 & \frac{\mathrm{N}}{\mathrm{Rm}} & 0 \\ 0 & -\frac{\mathrm{N}}{\mathrm{Re}} & 4i\frac{\mathrm{Ro}-\mathrm{Rb}}{\alpha n \mathrm{Rm}} & \frac{1}{\mathrm{Rm}} \\ \frac{\mathrm{N}}{\mathrm{Re}} & 0 & -\frac{1}{\mathrm{Rm}} & 0 \end{pmatrix}. \tag{4.6}$$

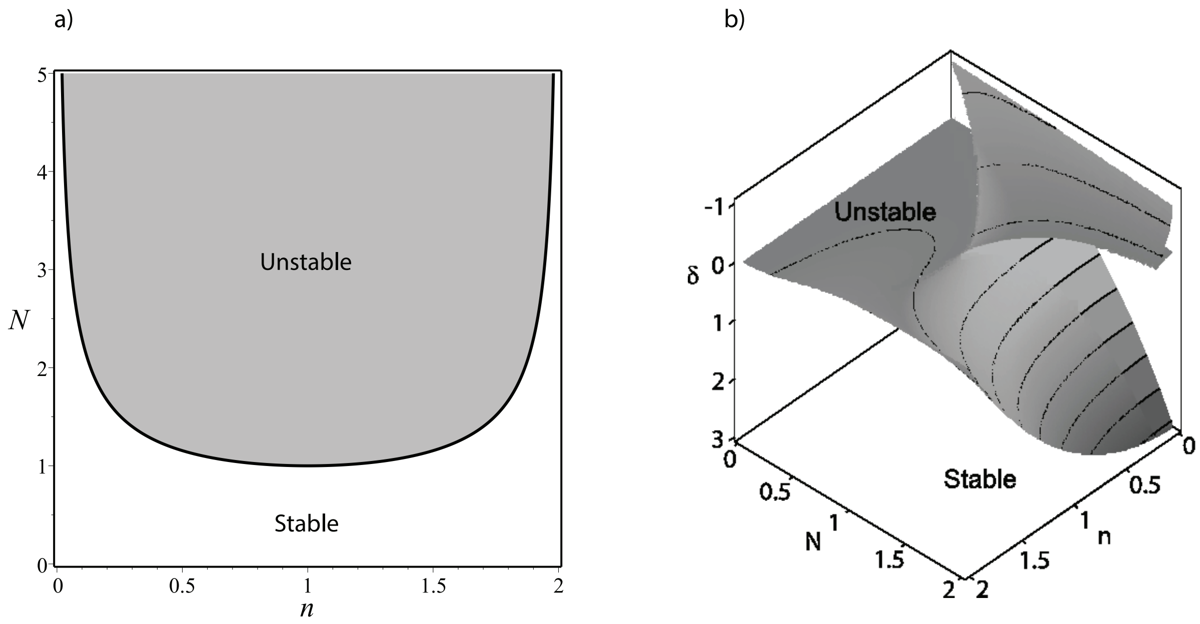

Fig. 2. (a) The planar stability diagram of the ideal system under the constraint $\delta := \mathrm{Ro} - \mathrm{Rb}\mathrm{N}^2 = 0$ with the boundary (5.5) is a cross-section of the full stability diagram (b) with the boundary (5.6) that has a Swallowtail singularity at $n = 1$, $\mathrm{N} = 1$, and $\delta = 0$.

5. Local linear stability of the ideal system

The ideal system (4.3) without viscosity and resistivity has the following characteristic polynomial

$$\begin{aligned} p(\lambda) &= \lambda^4 + 4in\lambda^3 + \left(2\mathrm{N}^2n^2 - 6n^2 + 4 + 4\delta\right)\lambda^2 \\ &+ 4in\left(2\delta + (n^2-2)(\mathrm{N}^2-1)\right)\lambda + n^2(\mathrm{N}^2-1)\left(4\delta + (n^2-4)(\mathrm{N}^2-1)\right), \end{aligned} \quad (5.1)$$

where $\delta = \mathrm{Ro} - \mathrm{Rb}\mathrm{N}^2$.

The dispersion relation corresponding to (5.1) possesses a compact representation [21, 34, 35, 47, 64]

$$4\delta((i\lambda - n)^2 - n^2\mathrm{N}^2) + 4(i\lambda - n + n\mathrm{N}^2)^2 - ((i\lambda - n)^2 - n^2\mathrm{N}^2)^2 = 0. \quad (5.2)$$

If $\delta = 0$, i.e. $\mathrm{Ro} = \mathrm{Rb}\mathrm{N}^2$, then the equation (5.2) simplifies and its roots are

$$\lambda_{1,2} = -i(n+1) \pm i\sqrt{\mathrm{N}^2(n+1)^2 + 1 - \mathrm{N}^2}, \quad (5.3)$$

$$\lambda_{3,4} = -i(n-1) \pm i\sqrt{\mathrm{N}^2(n-1)^2 + 1 - \mathrm{N}^2}. \quad (5.4)$$

These roots are shown in Fig. 1 for different values of N. For $0 \le \mathrm{N} < 1$ the eigenvalues are imaginary and simple at all $0 < n \le 2$; at $n = 0$ there exists a double zero eigenvalue with the Jordan block and a pair of simple imaginary eigenvalues, Fig. 1(a). At $\mathrm{N} = 1$ there exist a double zero eigenvalue which is semi-simple at all $0 \le n \le 2$ but $n = 1$ where it has a Jordan block of order 2. The other two eigenvalue branches are formed by simple imaginary eigenvalues, Fig. 1(b), and correspond to $\mathrm{N} = 1$ and $\mathrm{Ro} = \mathrm{Rb}$, which includes the Chandrasekhar equipartition solution. At $\mathrm{N} > 1$ a bubble of complex-conjugate eigenvalues originates, Fig. 1(c,d), if n belongs to a region bounded by the curve

$$\mathrm{N} = \frac{1}{\sqrt{1-(n-1)^2}} \quad (5.5)$$

that is shown in Fig. 2(a).

At the boundary (5.5) the eigenvalues are double imaginary with the Jordan block of order 2. Therefore, at its intersection the marginal stability is lost via the Hamilton-Hopf bifurcation, Fig. 1(c,d). At $\mathrm{N} = 1$ and $n = 1$, the double eigenvalue with the Jordan block is zero. Its splitting at the fixed $\mathrm{N} = 1$ and at the

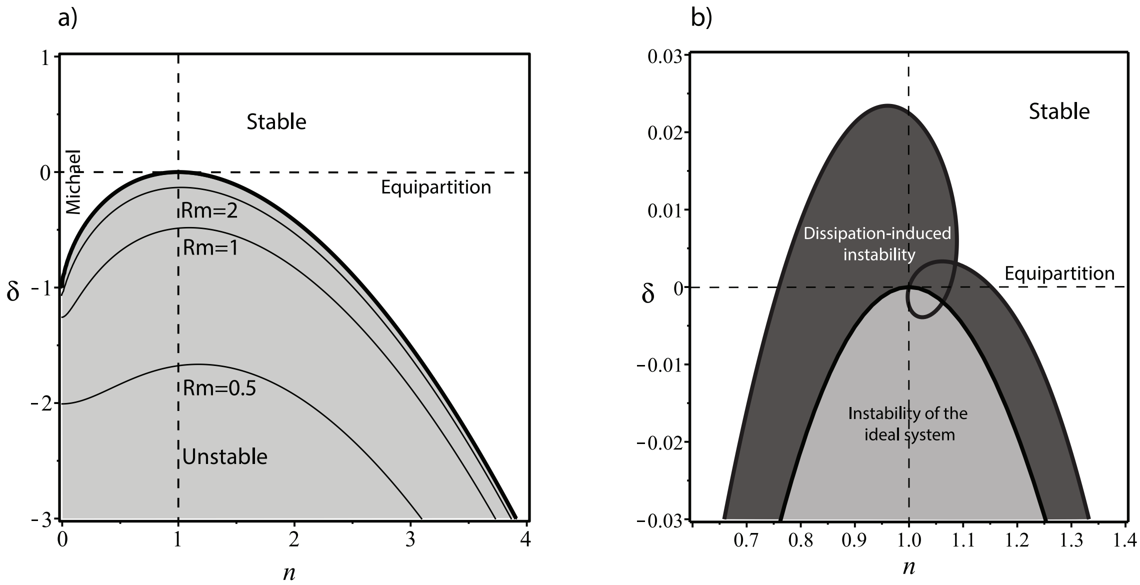

Fig. 3. (a) At $\mathrm{N} = 1$ the instability domain (light grey area) of the ideal system with the boundary (5.7) and the boundaries (6.3) of the instability domains of the dissipative system with $\mathrm{Re} = \mathrm{Rm}$ that tend to that of the ideal system when $\mathrm{Rm} \to \infty$. (b) At $\mathrm{N} = 1$ the instability domain of the ideal system (light grey) in comparison with the instability domain of the dissipative system (dark grey) at $\mathrm{Re} = 10^6$, $\mathrm{Rm} = 10$, and $\mathrm{Pm} = 10^{-5}$ show the dissipation-induced instability.

varying n is linear with respect to n, which is degenerate because it happens along a tangent direction to the stability boundary. Note that such type of splitting as well as the corresponding metamorphoses of the eigenvalue curves shown in Fig. 1 where described analytically in [25, 33].

In Fig. 2(a) only part of the stability diagram of the polynomial (5.1) is shown under the constraint $\delta = 0$. To get an idea what happens when $\delta \neq 0$ we consider the discriminant set of the polynomial (5.1):

$$\begin{aligned} 4\delta^5 &+ (\mathrm{N}^2 n^2 - 4\mathrm{N}^2 + 16)\delta^4 + (8\mathrm{N}^4 n^2 + 12\mathrm{N}^2 n^2 - 12\mathrm{N}^2 + 24)\delta^3 \\ &+ (2\mathrm{N}^6 n^4 - 8\mathrm{N}^6 n^2 + 2\mathrm{N}^4 n^4 - 22\mathrm{N}^4 n^2 + 22\mathrm{N}^2 n^2 - 12\mathrm{N}^2 + 16)\delta^2 \\ &+ 4(\mathrm{N}^2 - 1)(\mathrm{N}^6 n^4 - 2\mathrm{N}^4 n^4 + 5\mathrm{N}^4 n^2 - 3\mathrm{N}^2 n^2 - 1)\delta \\ &+ \mathrm{N}^2 n^2 (\mathrm{N}^2 - 1)^2 (\mathrm{N}^4 n^4 - 4\mathrm{N}^4 n^2 + 2\mathrm{N}^2 n^2 + 1) = 0. \end{aligned} \tag{5.6}$$

Equation (5.6) defines a singular surface in the space of parameters n, N, and δ with the Swallowtail singularity at $n = 1$, $\mathrm{N} = 1$, and $\delta = 0$, Fig. 2(b). The smooth parts of the surface correspond to double imaginary eigenvalues with the Jordan block of order two; at the two cuspidal edges the eigenvalues are triple imaginary with the Jordan block of order 3.

For the Chandrasekhar equipartition solution we have $\mathrm{N} = 1$ and $\delta = \mathrm{Ro} - \mathrm{Rb} = 0$. Therefore, it is instructive to consider the cross-section of the full stability diagram shown in Fig. 2(b) by the plane $\mathrm{N} = 1$. From (5.6) we derive the boundary in the (n, δ) plane:

$$n = \frac{1}{4}\sqrt{-2\delta^2 - 40\delta + 16 \pm 2\sqrt{\delta(\delta - 8)^3}}. \tag{5.7}$$

The result we plot in Fig. 3(a), where the planar instability domain of the ideal system is shown in light grey. Notice stabilization at $n = 0$ when $\delta > -1$ in accordance with the Michael criterion [45]. On the other hand the branch of the stability boundary at $n > 1$ has the following asymptotic representation at

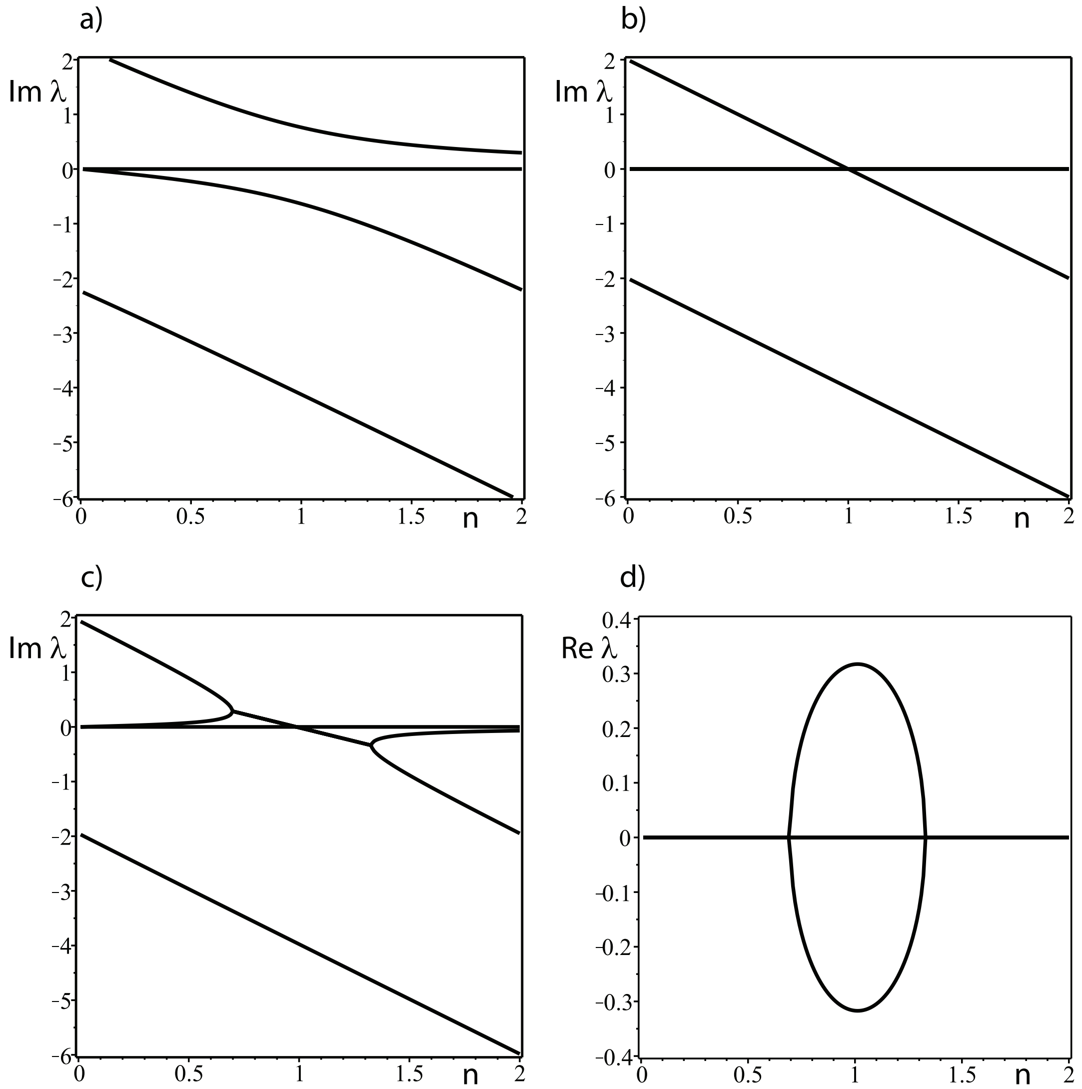

Fig. 4. Frequencies and growth rates of the roots of the dispersion relation (5.2) under the constraint N = 1 when (a) Ro = −0.75 and Rb = −1 ($\delta = 0.25$), (b) Ro = −0.75 and Rb = −0.75 ($\delta = 0$), and (c,d) Ro = −0.75 and Rb = −0.7 ($\delta = -0.05$).

$\delta \to -\infty$:

$$n = 2\sqrt{-\delta} + O\left(\frac{1}{\sqrt{-\delta}}\right), \tag{5.8}$$

in full agreement with the threshold of azimuthal magnetorotational instability (1.10) in the ideal case [47, 64].

The line $\delta = 0$, which the equipartition solution belongs to, is in the stability domain of the ideal system, Fig. 3(a). The corresponding curves of imaginary eigenvalues are shown in Fig. 4(a) and demonstrate crossing at $n = 1$ where there exist a pure imaginary eigenvalue, a simple zero eigenvalue, and a double zero eigenvalue with the Jordan block of order 2. At $\delta > 0$ the crossing transforms into the avoided crossing shown in Fig. 4(b) with all the eigenvalues imaginary (marginal stability). At $\delta < 0$ the eigenvalue curves merge with the origination of the bubble of complex eigenvalues, see Fig. 4(c,d). The instability takes place through the Hamilton-Hopf bifurcation at the threshold (5.7).

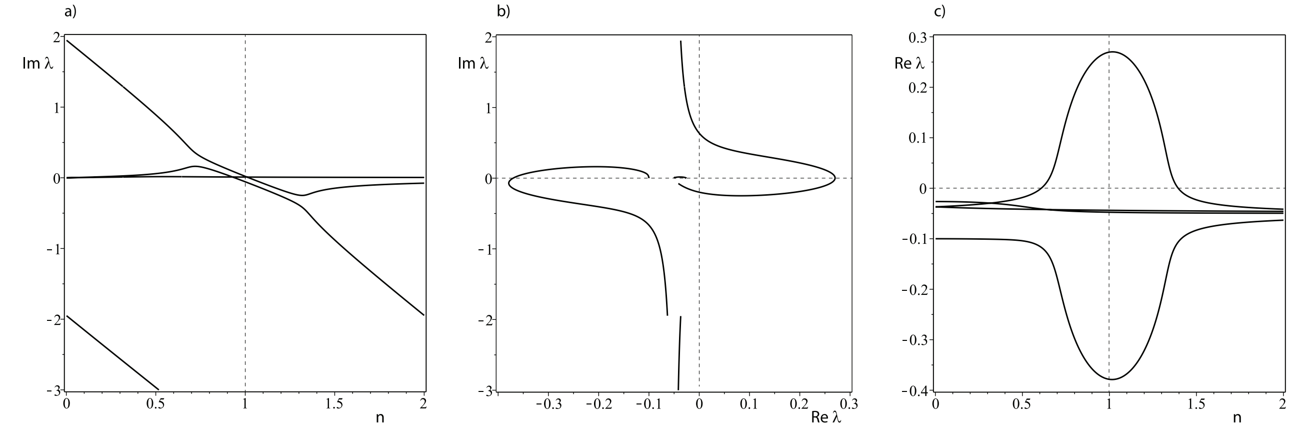

Fig. 5. Frequencies and growth rates of the dissipative system at $\mathrm{Re} = 10^6$, $\mathrm{Rm} = 10$, $\mathrm{Pm} = 10^{-5}$, and $\mathrm{Ro} = -0.75$, $\mathrm{Rb} = -0.7$, $\mathrm{N} = 1$. Enlarging the interval of instability due to imperfect merging of modes in the presence of non-equal Re and Rm.

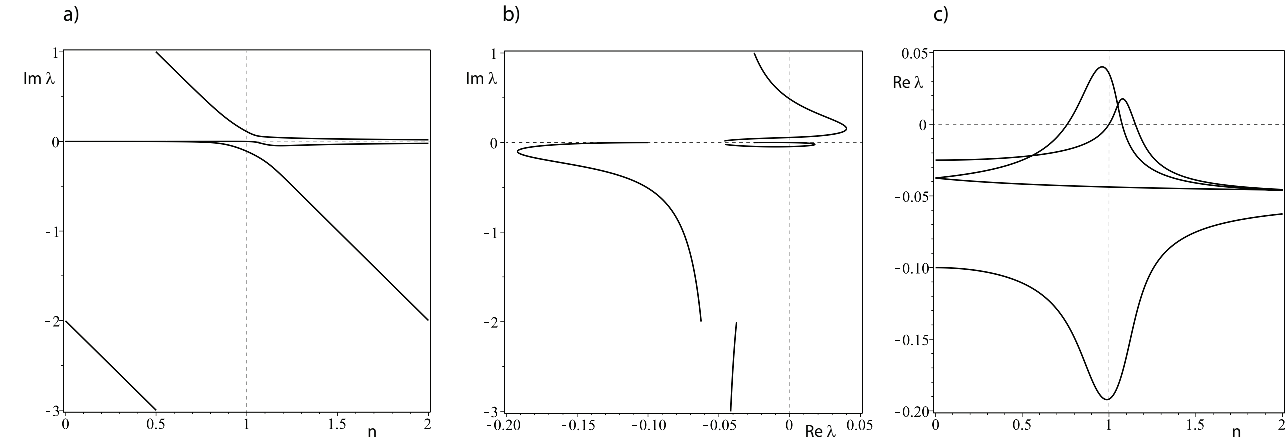

Fig. 6. Frequencies and growth rates of the dissipative system at $\mathrm{Re} = 10^6$, $\mathrm{Rm} = 10$, $\mathrm{Pm} = 10^{-5}$, $\mathrm{Ro} = -0.75$, $\mathrm{Rb} = -0.75$, $\mathrm{N} = 1$. Avoided crossing of the frequencies and positive growth rates of the equipartition solution.

6. Azimuthal MRI at low Pm as a dissipation-induced instability

Let us consider the influence of viscosity and resistivity of the fluid on the threshold of instability of the ideal system. First of all we observe that in case when $\mathrm{Ro} = \mathrm{Rb}\mathrm{N}^2$ and $\mathrm{Re} = \mathrm{Rm}$, the roots of the characteristic polynomial (3.7) can be found explicitly

$$\lambda_{1,2} = -i(n+1) - \frac{1}{\mathrm{Rm}} \pm i\sqrt{\mathrm{N}^2(n+1)^2 + 1 - \mathrm{N}^2}, \tag{6.1}$$

$$\lambda_{3,4} = -i(n-1) - \frac{1}{\mathrm{Rm}} \pm i\sqrt{\mathrm{N}^2(n-1)^2 + 1 - \mathrm{N}^2}. \tag{6.2}$$

This means that at $\mathrm{Pm} = 1$ the pure imaginary eigenvalues (5.3) and (5.4) are shifted by the dissipation to the left in the complex plane (asymptotic stability). Moreover, dissipation makes the domain of instability smaller when the hydrodynamic and magnetic Reynolds numbers are equal.

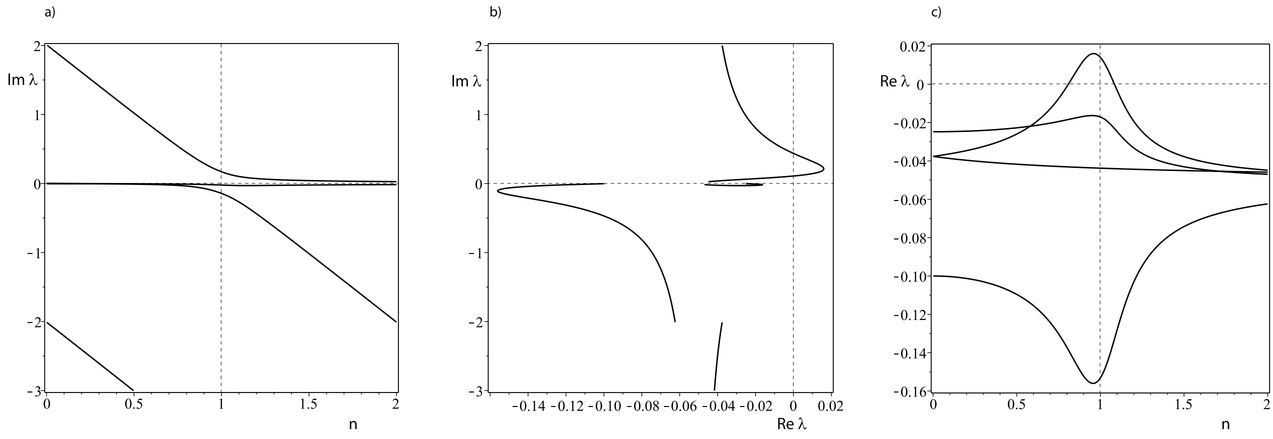

Fig. 7. Frequencies and growth rates of the dissipative system at $\mathrm{Re} = 10^6$, $\mathrm{Rm} = 10$, $\mathrm{Pm} = 10^{-5}$, $\mathrm{Ro} = -0.75$, $\mathrm{Rb} = -0.76$, $\mathrm{N} = 1$. Dissipation-induced instability in the area of parameters that was stable in case of the ideal system.

We demonstrate this by applying the Bilharz criterion [5] to the polynomial (3.7) and assuming $\mathrm{Re} = \mathrm{Rm}$, $\mathrm{N} = 1$, and $\delta = \mathrm{Ro} - \mathrm{Rb}$ in order to obtain the stability boundary

$$4\delta^3 + \left(n^2 + 12 + \frac{9}{\mathrm{Rm}^2}\right)\delta^2 + 2\left(10n^2 + 6 + \frac{3n^2}{\mathrm{Rm}^2} + \frac{9}{\mathrm{Rm}^2} + \frac{3}{\mathrm{Rm}^4}\right)\delta + \left(4 + \frac{1}{\mathrm{Rm}^2}\right)\left((n+1)^2 + \frac{1}{\mathrm{Rm}^2}\right)\left((n-1)^2 + \frac{1}{\mathrm{Rm}^2}\right) = 0. \quad (6.3)$$

As is seen in Fig. 3(a) the planar stability domain of the system with dissipation at $\mathrm{Pm} = 1$ is smaller than the instability domain of the ideal system and tends to it with the increase in Rm when the magnetic Reynolds number tends to infinity.

What happens with the stability threshold of the ideal system when the proportion between the viscosity and resistivity is smaller than 1 and, especially, when $\mathrm{Pm} \ll 1$? In Fig. 3(b) we plot the domain of instability (dark grey) of the viscous and resistive system with $\mathrm{N} = 1$ and $\mathrm{Re} \gg \mathrm{Rm}$ so that $\mathrm{Pm} = 10^{-5}$. The domain in light grey is a part of the instability region of the ideal system shown in light grey in Fig. 3(a). The dark grey area in Fig. 3(b) indicates instability for the values of parameters that correspond to the marginally stable ideal system. The line $\delta = 0$, which the Chandrasekhar equipartition solution belongs to, is intersecting the domain of dissipation-induced instability. With the Pm kept fixed and Re and Rm increasing to infinity, the domain of dissipation-induced instability extends and tends to some limit. For example, at $\mathrm{Ro} = -\frac{3}{4}$ the difference $\delta := \mathrm{Ro} - \mathrm{Rb}$ cannot increase beyond the value $-\frac{3}{4} + \frac{25}{32} = \frac{1}{32} = 0.03125$. The latter can be reached only in the inductionless limit $\mathrm{Pm} = 0$ [31, 34, 35]. The eigenvalues of the dissipative system shown in Fig. 5-7 illustrate the extension of the domain of marginal stability under the influence of two different dissipative mechanisms: viscosity and resistivity. Contrary to the case when the coefficients of viscosity and resistivity are equal, the prevalence of resistivity over viscosity indeed causes the azimuthal magnetorotational instability at the region of parameters where in the ideal system AMRI is prohibited. In particular, non-equal viscosity and resistivity destabilize the Chandrasekhar equipartition solution. It would be interesting to perform a further study of this effect using the fundamental symmetry of the Hamiltonian system in order to classify the modes of the ideal system and to understand how the modes with positive and negative symplectic sign [33, 62] react on viscous and resistive perturbations. We leave this for a future work.

Acknowledgement

I am grateful to S. Dobrokhotov for helpful discussions.

REFERENCES

1. V. I. Arnold, "On matrices depending on parameters," *Russian Mathematical Surveys,* **26**, 29–43 (1971).
2. S. A. Balbus, J. F. Hawley, "A powerful local shear instability in weakly magnetized disks 1. Linear analysis," *Astrophys. J.,* **376**, 214–222 (1991).
3. S. A. Balbus, J. F. Hawley, "A powerful local shear instability in weakly magnetized disks 4. Nonaxisymmetric perturbations," *Astrophys. J.,* **400**, 610–621 (1992).
4. V. V. Beletsky, E. M. Levin, "Stability of a ring of connected satellites," *Acta Astron.,* **12**, 765–769 (1985).
5. H. Bilharz, "Bemerkung zu einem Satze von Hurwitz," *Z. Angew. Math. Mech.,* **24**, 77–82 (1944).
6. A. M. Bloch, P. S. Krishnaprasad, J. E. Marsden, T. S. Ratiu, "Dissipation-induced instabilities," *Annales de L'Institut Henri Poincare - Analyse Non-Lineaire,* **11**, 37–90 (1994).
7. O. I. Bogoyavlenskij, "Unsteady equipartition MHD solutions," *J. Math. Phys.,* **45**, 381–390 (2004).
8. S. Boldyrev, D. Huynh, V. Pariev, "Analog of astrophysical magnetorotational instability in a Couette-Taylor flow of polymer fluids," *Phys. Rev. E,* **80**, 066310 (2009).
9. V. V. Bolotin, *Nonconservative Problems of the Theory of Elastic Stability*, Pergamon Press, Oxford, London, New York, Paris (1963).
10. O. Bottema, "The Routh-Hurwitz condition for the biquadratic equation," *Indag. Math.,* **18**, 403–406 (1956).
11. T. J. Bridges, F. Dias, "Enhancement of the Benjamin-Feir instability with dissipation," *Physics of Fluids,* **19**, 104104 (2007).
12. S. Chandrasekhar, "On the stability of the simplest solution of the equations of hydromagnetics," *Proc. Natl. Acad. Sci. U.S.A.,* **42**, 273–276 (1956).
13. S. Chandrasekhar, "The stability of non-dissipative Couette flow in hydromagnetics," *Proc. Natl. Acad. Sci. U.S.A.,* **46**, 253–257 (1960).
14. S. Chandrasekhar, *Hydrodynamic and hydromagnetic stability*, Oxford University Press, Oxford, UK (1961).
15. S. Chandrasekhar, *A scientific autobiography: S. Chandrasekhar, K. C. Wali, ed.*, World Scientific, Singapore, p. 38 (2010).
16. S. Dobrokhotov, A. Shafarevich, "Parametrix and the asymptotics of localized solutions of the Navier-Stokes equations in R^3, linearized on a smooth flow," *Math. Notes,* **51**, 47–54 (1992).
17. F. Ebrahimi, B. Lefebvre, C. B. Forest, A. Bhattacharjee, "Global Hall-MHD simulations of magnetorotational instability in the plasma Couette flow experiment," *Phys. Plasmas,* **18**, 062904 (2011).
18. B. Eckhardt, D. Yao, "Local stability analysis along Lagrangian paths," *Chaos, Solitons and Fractals*, **5**(11), 2073–2088 (1995).
19. K. S. Eckhoff, "On stability for symmetric hyperbolic systems, I.," *J. Differ. Equ.,* **40**, 94–115 (1981).
20. K. S. Eckhoff, "Linear waves and stability in ideal magnetohydrodynamics," *Phys. Fluids,* **30**, 3673–3685 (1987).
21. S. Friedlander, M. M. Vishik, "On stability and instability criteria for magnetohydrodynamics," *Chaos,* **5**, 416–423 (1995).
22. S. V. Golovin, M. K. Krutikov, "Complete classification of stationary flows with constant total pressure of ideal incompressible infinitely conducting fluid," *J. Phys. A: Math. Theor.,* **45**, 235501 (2012).
23. H. Ji, S. Balbus, "Angular momentum transport in astrophysics and in the lab," *Physics Today, August 2013*, 27–33 (2013).
24. P. L. Kapitsa, "Stability and passage through the critical speed of the fast spinning rotors in the presence of damping," *Z. Tech. Phys.,* **9**, 124–147 (1939).
25. O. N. Kirillov, A. P. Seyranian, "Metamorphoses of characteristic curves in circulatory systems," *Journal of Applied Mathematics Mechanics*, **66**(3), 371–385 (2002).

26. O. N. Kirillov, "Campbell diagrams of weakly anisotropic flexible rotors," *Proc. R. Soc. Lond. Ser. A Math. Phys. Eng. Sci.,* **465**, 2703–2723 (2009).
27. O. N. Kirillov, F. Verhulst, "Paradoxes of dissipation-induced destabilization or who opened Whitney's umbrella?" *Z. Angew. Math. Mech.*, **90**(6), 462–488 (2010).
28. O. N. Kirillov, F. Stefani, "On the relation of standard and helical magnetorotational instability," *Astrophys. J.,* **712**, 52–68 (2010).
29. O. N. Kirillov, F. Stefani, "Standard and helical magnetorotational instability: How singularities create paradoxal phenomena in MHD," *Acta Appl. Math.*, **120**, 177–198 (2012).
30. O. N. Kirillov, F. Stefani, Y. Fukumoto, "A unifying picture of helical and azimuthal MRI, and the universal significance of the Liu limit," *The Astrophysical Journal*, **756**(83) (2012).
31. O. N. Kirillov, F. Stefani, "Extending the range of the inductionless magnetorotational instability," *Phys. Rev. Lett.,* **111**, 061103 (2013).
32. O. N. Kirillov, "Stabilizing and destabilizing perturbations of PT-symmetric indefinitely damped systems," *Phil. Trans. R. Soc. A,* **371**, 20120051 (2013).
33. O. N. Kirillov, *Nonconservative stability problems of modern physics*, De Gruyter Studies in Mathematical Physics 14, De Gruyter, Berlin, Boston (2013).
34. O. N. Kirillov, F. Stefani, Y. Fukumoto, "Instabilities of rotational flows in azimuthal magnetic fields of arbitrary radial dependence," *Fluid Dyn. Res.,* **46**, 031403 (2014).
35. O. N. Kirillov, F. Stefani, Y. Fukumoto, "Local instabilities in magnetized rotational flows: A short-wavelength approach," *J. Fluid Mech.,* **760**, 591–633 (2014).
36. E. R. Krueger, A. Gross, R. C. Di Prima, "On relative importance of Taylor-vortex and non-axisymmetric modes in flow between rotating cylinders," *J. Fluid Mech.*, **24**(3), 521–538 (1966).
37. R. Krechetnikov, J. E. Marsden, "Dissipation-induced instabilities in finite dimensions," *Rev. Mod. Phys.,* **79**, 519–553 (2007).
38. V. V. Kucherenko, A. Kryvko, "Interaction of Alfvén waves in the linearized system of magnetohydrodynamics for an incompressible ideal fluid," *Russ. J. Math. Phys.*, **20**(1), 56–67 (2013).
39. M. J. Landman, P. G. Saffman, "The three-dimensional instability of strained vortices in a viscous fluid," *Phys. Fluids,* **30**, 2339–2342 (1987).
40. W. F. Langford, Hopf meets Hamilton under Whitney's umbrella, in: S. N. Namachchivaya, (ed.), IUTAM Symposium on Nonlinear Stochastic Dynamics. Proceedings of the IUTAM Symposium, Monticello, IL, USA, Augsut 26-30, 2002, Solid Mech. Appl. 110, pp. 157–165, Kluwer, Dordrecht (2003).
41. H. N. Latter, H. Rein, G. I. Ogilvie, "The gravitational instability of a stream of coorbital particles," *Mon. Not. R. Astron. Soc.,* **423**, 1267–1276 (2012).
42. W. Liu, J. Goodman, I. Herron, H. Ji, "Helical magnetorotational instability in magnetized Taylor-Couette flow," *Phys. Rev. E*, **74**(5), 056302 (2006).
43. R. S. MacKay, "Movement of eigenvalues of Hamiltonian equilibria under non-Hamiltonian perturbation," *Phys. Lett. A,* **155**, 266–268 (1991).
44. J. H. Maddocks, M. L. Overton, "Stability theory for dissipatively perturbed Hamiltonian-systems," *Comm. Pure Appl. Math.,* **48**, 583–610 (1995).
45. D. H. Michael, "The stability of an incompressible electrically conducting fluid rotating about an axis when current flows parallel to the axis," *Mathematika,* **1**, 45–50 (1954).
46. D. Montgomery, "Hartmann, Lundquist, and Reynolds: The role of dimensionless numbers in non-linear magnetofluid behavior," *Plasma Phys. Control. Fusion,* **35**, B105–B113 (1993).
47. G. I. Ogilvie, J. E. Pringle, "The non-axisymmetric instability of a cylindrical shear flow containing an azimuthal magnetic field," *Mon. Not. R. Astron. Soc.,* **279**, 152–164 (1996).
48. G. I. Ogilvie, M. R. E. Proctor, "On the relation between viscoelastic and magnetohydrodynamic flows and their instabilities," *J. Fluid Mech.,* **476**, 389–409 (2003).
49. G. I. Ogilvie, A. T. Potter, "Magnetorotational-type instability in Couette-Taylor flow of a viscoelastic polymer liquid," *Phys. Rev. Lett.,* **100**, 074503 (2008).

50. J. W. S. Rayleigh, “On the dynamics of revolving fluids,” *Proc. R. Soc. Lond. A,* **93**, 148–154 (1917).
51. G. Rüdiger, M. Gellert, M. Schultz, R. Hollerbach, “Dissipative Taylor–Couette flows under the influence of helical magnetic fields,” *Phys. Rev. E,* **82**, 016319 (2010).
52. G. Rüdiger, L. Kitchatinov, R. Hollerbach, *Magnetic Processes in Astrophysics*, Wiley-VCH (2013).
53. G. Rüdiger, M. Gellert, M. Schultz, R. Hollerbach, F. Stefani, “The azimuthal magnetorotational instability (AMRI),” *Mon. Not. R. Astron. Soc.,* **438**, 271–277 (2014).
54. M. Seilmayer, V. Galindo, G. Gerbeth, T. Gundrum, F. Stefani, M. Gellert, G. Rüdiger, M. Schultz, R. Hollerbach, “Experimental evidence for non-axisymmetric magnetorotational instability in an azimuthal magnetic field,” *Phys. Rev. Lett.,* **113**, 024505 (2014).
55. D. M. Smith, “The motion of a rotor carried by a flexible shaft in flexible bearings,” *Proc. R. Soc. Lond. A,* **142**, 92–118 (1933).
56. J. Squire, A. Bhattacharjee, “Nonmodal growth of the magnetorotational instability,” *Phys. Rev. Lett.,* **113**, 025006 (2014).
57. F. Stefani, A. Gailitis, G. Gerbeth, “Magnetohydrodynamic experiments on cosmic magnetic fields,” *Z. Angew. Math. Mech.,* **88**, 930–954 (2008).
58. G. E. Swaters, “Modal interpretation for the Ekman destabilization of inviscidly stable baroclinic flow in the Phillips model,” *J. Phys. Oceanogr.,* **40**, 830–839 (2010).
59. S. A. Thorpe, W. D. Smyth, L. Li, “The efect of small viscosity and diffusivity on the marginal stability of stably stratified shear flows,” *J. Fluid Mech.,* **731**, 461–476 (2013).
60. E. P. Velikhov, Stability of an ideally conducting liquid flowing between cylinders rotating in a magnetic field,” *Sov. Phys. JETP-USSR,* **9**, 995–998 (1959).
61. M. Vishik, S. Friedlander, Asymptotic methods for magnetohydrodynamic instability,” *Quart. Appl. Math.,* **56**, 377–398 (1998).
62. V. A. Yakubovich, V. M. Starzhinskii, *Linear Differential Equations with Periodic Coefficients*, vols. 1 and 2, Wiley, New York (1975).
63. H. Ziegler, “Die Stabilitätskriterien der Elastomechanik,” *Archive Appl. Mech.,* **20**, 49–56 (1952).
64. R. Zou, Y. Fukumoto, “Local stability analysis of the azimuthal magnetorotational instability of ideal MHD flows,” *Prog. Theor. Exp. Phys.*, 113J01 (2014).

Oleg N. Kirillov
Helmholtz-Zentrum Dresden-Rossendorf
E-mail: `o.kirillov@hzdr.de`